A comprehensive study of the influence of non-covalent interactions on electron density redistribution during the reaction between acetic acid and methylamine

Olivier Aroule, Emilie-Laure Zins

A Comprehensive Study of the Influence of Non-Covalent Interactions on Electron Density Redistribution during the Reaction between Acetic Acid and Methylamine

Olivier Aroule,[1] Emilie-Laure Zins[1,*]

1. Sorbonne Université, Laboratoire "De la Molécule aux Nano-objets : Réactivité, Interactions et Spectroscopies", MONARIS, F75005 Paris, France

Contact: emilie-laure.zins@sorbonne-universite.fr ORCID: 0000-0002-2157-6696

Abstract

Context: A chemical reaction can be described, from a physicochemical perspective, as a redistribution of electron density. Additionally, non-covalent interactions locally modify the electron density distribution. This study aims to characterize the modification of reactivity caused by the presence of non-covalent interactions such as hydrogen bonds, in a reaction involving the formation of two bonds and the breaking of two others: $CH_3COOH + NH_2CH_3 \rightarrow CH_3CONHCH_3$.

Methods: In this work, we will follow the how a reaction mechanism involving the formation of two chemical bonds and the breaking of two other chemical bonds is affected by non-covalent interaction. To this end, the reaction force will be used to define the region of the reagents, the region of the transition state, and the region of the products. We will analyze the redistributions of electron density and electron pairs in each of the regions of the reaction mechanisms, using QTAIM and ELF ' topological analyses, respectively, for the reaction between methylamine and acetic acid, in the presence of 0 to 4 water molecules. DFT calculations were carried out at the LC-ωPBE/6-311++G(d,p) + GD3BJ level along the intrinsic reaction coordinate of the one-step reaction leading to the formation of methylacetamide.

Keywords

Non-covalent interactions,

Reaction mechanism,

Electronic redistribution,

QTAIM topological analysis,

ELF topological analysis

I. Introduction

A growing chemical diversity is being evidenced in interstellar clouds with the help of the most powerful telescopes. Generally, two families of processes are considered to explain the synthesis of these molecules in extremely cold and dilute environments: [1-4] i) solid-phase processes on the surface of ice grains that could significantly lower energy barriers, and ii) gas-phase processes. Despite numerous studies on the subject, we are still far from explaining the entire chemical diversity evidenced by the telescopes. Among others, the reactions leading to the formation of molecules containing the 4 C, H, O and N atoms essential for life as we know it are the subject of numerous laboratory studies, to determine whether such molecules could be formed under interstellar conditions. In particular, the Strecker synthesis has been extensively studied: the first stages of this reaction lead to the formation of an aminoalcohol R-CH(OH)-NH_2 from ammonia and an aldehyde; then the dehydration of the thus formed aminoalcohol lead to the formation of an imine RCHNH (Reaction1): [5]

NH_3 + R-C(O)H → R-CH(OH)-NH_2 (1)

It has been shown [6] that the presence of a few water molecules can significantly lower the energy barrier associated with this reaction, whether the water molecules act as an active or passive catalyst. Without the presence of a water molecule, the energy barrier for the reaction between CH_2=O and NH_3 is 140 kJ/mol, whereas the addition of a single water molecule as a passive catalyst lowers the energy barrier by around 20 kJ/mol. When a water molecule is added as an active catalyst, the energy barrier is lowered by around 80 kJ/mol.

The role of a few explicit water molecules in the mechanisms leading to the formation of peptide-type bonds (amide bonds) has also been extensively studied in the context of the chemistry of the interstellar medium. Without a molecule of water, the formation of formamide HC(O)-NH_2 by reaction between acetic acid and ammonia can proceed according to two types of mechanism: a concerted, one-step mechanism, and a two-step mechanism with the formation of a diol as a reaction intermediate (Reaction 2). [7] The energy barriers associated with this reaction are of 33.1 and 32.2 kcal/mol (138.1 and 133.9 in kJ/mol respectively) for the first and second steps of the two-step mechanism, respectively, and 34.9 kcal/mol (142.2 kJ/mol) for the one-step mechanism. [7]

NH_3 + CH_2COOH → NH_2-C(O)H + H_2O (2)

The role of a few explicit water molecules as a catalyst in this peptide bond formation reaction has been demonstrated in particular in the dimerisation process of glycine (Reaction 3) when one to nine water molecules are added: the reaction is favoured by an increasing number of water molecules; this has been attributed to the stabilisation of the product by non-covalent interactions with the water molecules. [8]

2 NH_2-CH_2-C(O)OH → NH_2- CH_2-C(O)-NH- CH_2-C(O)OH + H_2O (3)

The role of water as a catalyst in the reaction to form a peptide-type bond has also been demonstrated in the case of the reaction to form acetamide from nitriles (Reaction4):

R-CN + H_2O → HC(OH)NH → HC(O)NH_2 (4)

The energetic barrier associated with this reaction is strongly lowered in the presence of an acidic water cluster $(H_2O)_{32}(H_3O)^+$. [9] It has also been shown that the role of water as a catalyst in these reactions can be demonstrated as soon as one or two molecules of water are taken into account, as in the case of the comparative study of the reaction of HCN and HNC with the OH radical, in the presence of 0 to 6 molecules of water. [10]

The effect of an amorphous solid water (ASW) surface on the reaction energetics was also thoroughly investigated. It has thus been shown that ice water dust mantles activate Strecker-type reactions, [11] as well as the reaction for the formation of aminoacetonitrile, [12] among others. Recently, ab initio molecular dynamics calculations have been used to identify catalytic sites on ASW in the case of the synthesis of aminoethanol. [13] Several studies have investigated different reaction pathways for the formation of formamide on realistic ASW surfaces. [14,15]

From a more fundamental point of view, any chemical reaction involves a redistribution of electron density leading to the breaking of some bonds and/or the formation of others. Among others, the following tools have been developed to describe this electronic redistribution:

- reaction force to define the region of reactants, transition states, and products along the reaction coordinate, [16-17-18]
- geometric analysis to characterize the evolution of different chemical bonds along the reaction path,
- topological analysis of the electron density using the Quantum Theory of Atoms in Molecules (QTAIM) approach to characterize electronic redistribution along the reaction path, [19-21]
- topological analysis of the Electron Localization Function (ELF) for an interpretation in terms of electron pairs and Lewis structures at key points along the reaction path. [22-24]

It is these approaches that will be used here to study how the presence of 1 to 4 water molecules modifies the electronic redistribution, and therefore the formation and breaking of bonds, in the case of the formation of methylacetamide, CH_3-C(O)-NH-CH_3 from acetic acid and methylamine. The reactants herein considered have all been detected in the SgRB2 cloud: acetic acid CH_3COOH, methylamine NH_2CH_3, and water. [25-27]The one step reaction $CH_3COOH + NH_2CH_3 \rightarrow CH_3CONHCH_3$ is chosen here as a prototype for this work because it involves the concomitant formation of bonds and breaking of two other bonds, allowing the tracking of the electronic redistributions that occur (scheme 1).

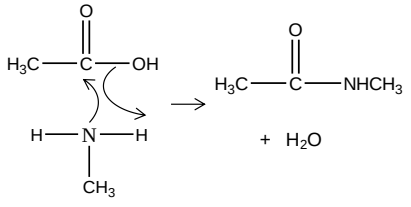

Scheme 1 : Formation of methylacetamide from acetic acid and methylamine in a one-step reaction.

II. Computational details

Geometry optimizations, frequency calculations, and calculations along the intrinsic reaction

All the calculations were performed using Gaussian16 revision C.01 software. [28] Density functional theory was used here. In coherence with a similar study reported in the literature on the same reaction, [29] we selected the hybrid functional LC-ωPBE [30-32] and the Pople triple-ξ basis set 6-311++G(d,p). The D3 version of Grimme's dispersion with Becke-Johnson damping was further used.[33] It has been shown in the literature that this level of calculation (LC-ωPBE + D3) provides an accurate description of this type of molecules. [34] The .wfn and .wfx cube files necessary for ELF and QTAIM topological analyses were generated at this stage. From the transition states already reported in the literature, calculations were performed along the intrinsic reaction coordinate. Energy, geometric, and topological analyses were then carried out on the various structures obtained along this intrinsic reaction coordinate. Reaction paths were followed by integrating the intrinsic reaction coordinate using the HPC algorithm. [35-37]

The energies of the stationary points have been calculated with reference to those of all the reactants taken separately (n(H_2O) + CH_3COOH + NH_2CH_3).

III. Theoretical framework

a. Reaction force

In the 2000s, A. Toro-Labbé et al. proposed the concept of reaction force to provide a framework for studying reaction mechanisms. [10-12; 38, 39] By analogy with physics, the reaction force is calculated as the negative derivative of the potential energy. This quantity defines three regions along the intrinsic reaction coordinate:

- the region of reactants, where pre-complexes can form through long-distance interactions between reactants. This region extends from the reactants to the intrinsic reaction coordinate at which the reaction force reaches its minimum value;
- the region of the transition state, where most of the electron density redistribution between reactants and products occurs. This region extends from the intrinsic reaction coordinate at which the reaction force reaches its minimum value to the intrinsic reaction coordinate at which the reaction force reaches its maximum value;
- and the region of products, mainly characterized by the relaxation of the formed species; This region extends from the intrinsic reaction coordinate at which the reaction force reaches its maximum value to the products.

The derivatives of the potential energies along the intrinsic reaction coordinate were calculated manually. Second derivatives were also calculated to determine the stability ($\frac{\partial^2 E}{\partial \zeta^2} \geq 0$) or instability ($\frac{\partial^2 E}{\partial \zeta^2} < 0$) of the system. [40] The primary objective of this analysis was to define the different regions of the reaction pathway for a geometric and topological analysis of the various bonds of interest in each region.

b. Topological analysis

QTAIM : [19-21] The QTAIM method was used to have information about the forming and the breaking of the different bonds that are evolving during the reaction. It is possible to do this type of analysis by investigating the electron density and the Laplacian of the electron density at the bond critical point (BCP). A bond critical point is a point when the gradient of the electron density vanishes. We'll use the sign of the Laplacian of the electron density as a marker of whether a bond is covalent ($\nabla^2\rho < 0$) or non-covalent ($\nabla^2\rho > 0$). The AIMALL software (version 19.10.12, [41]) was used for this analysis.

ELF :[22-24] Another tool that we used is based on the electron pairs: this method is called ELF for Electron Localization Function. This method can allow us to have information about the basin which can be core or valence basins whether they correspond to non-bonding or bonding doublets. [42] Valence basins V(X) are called monosynaptic basins and represent free electron pairs; and they are colored in orange. The valence basins V(X,Y) are called disynaptic basins: they represent the electron doublets of a bond, and they are colored in green. Basins colored in cyan are called monosynaptic protonated basins and include a hydrogen atom. [43] The core and valence basins may or may not be separated depending on the cutoff values that we used. In this paper, the ELF value was set at 0.89. These analyses were carried out with the TopChem2 software [44,45].

The approach combining reaction force analysis and topological analysis, will help us understand the driving force of the reaction and the role of microhydration on it. Two types of microhydration will be considered here: the microhydration of one of the reactants, and the most energetically favorable microhydration identified, which corresponds to a stabilization of the transition state by water molecules. [46]

Since the microhydration of acetic acid is energetically more favorable than that of methylamine, it is the microhydrated acetic acid that will react with methylamine in the case of a reaction between two partners. The stabilization of the transition state by microhydration leads to water molecules placed between acetic acid and methylamine. After identifying the structure of the microhydrated reagents and/or those of the transition states, an intrinsic reaction coordinates (IRC) calculation is carried out to identify the entire reaction path. Mechanisms involving proton relays by water molecules preferentially lead to two-step mechanisms, involving a diol as a reaction intermediate, and these mechanisms will not be discussed here.

First, we will analyze the reaction mechanism without water molecules. Then, we will study the influence of microhydration on acetic acid. Finally, we will study the influence of microhydration on the transition state.

IV. Results

a. Geometric analysis

The evolution of interatomic distances dA-B corresponding to the two bonds formed (dC-N, dO-H) and the two bonds broken (dN-H, dC-O) was determined along the reaction pathway. Additionally, and similar to the analysis of energy, we examined its derivative of the interatomic distances along the intrinsic reaction coordinate: $(\partial(\text{dA-B}))/\partial\zeta$, allowing for a better characterization of the changes in geometric distances. We consider the absolute value of this distance variation between points (n-1) and (n+1) along the intrinsic reaction coordinate.

b. Study of the Reaction Pathway in a Single Step without Water Molecule

The terms σ-holes and π-holes were introduced by Politzer et al. to characterize electrophilic regions located along the axis of a bond (σ-hole) or perpendicular to this axis (π-hole), respectively. [47-49] Thus, there is a π-hole at the carbonyl carbon atom of acetic acid, and σ-holes at the hydrogen atoms of the amine and carboxylic acid groups (see Supplementary Materials). The single-step reaction involves the formation of a non-covalent complex between the π-hole of the carbonyl carbon atom of acetic acid and the non-bonding pair of the nitrogen atom in methylamine (Figure 1A). The transition state allows for the formation of the C-N bond, the loss of the hydroxyl group, and the transfer of a proton from the transient structure to the hydroxyl group for the elimination of the water molecule (Fig. 1A). The IRC calculation confirms that this is a single-step process, characterized by the reactant region ($-5.2 < \zeta < -0.47$), the transition state region ($-0.47 < \zeta < 0.44$), and the product region ($0.44 < \zeta < 5.2$).

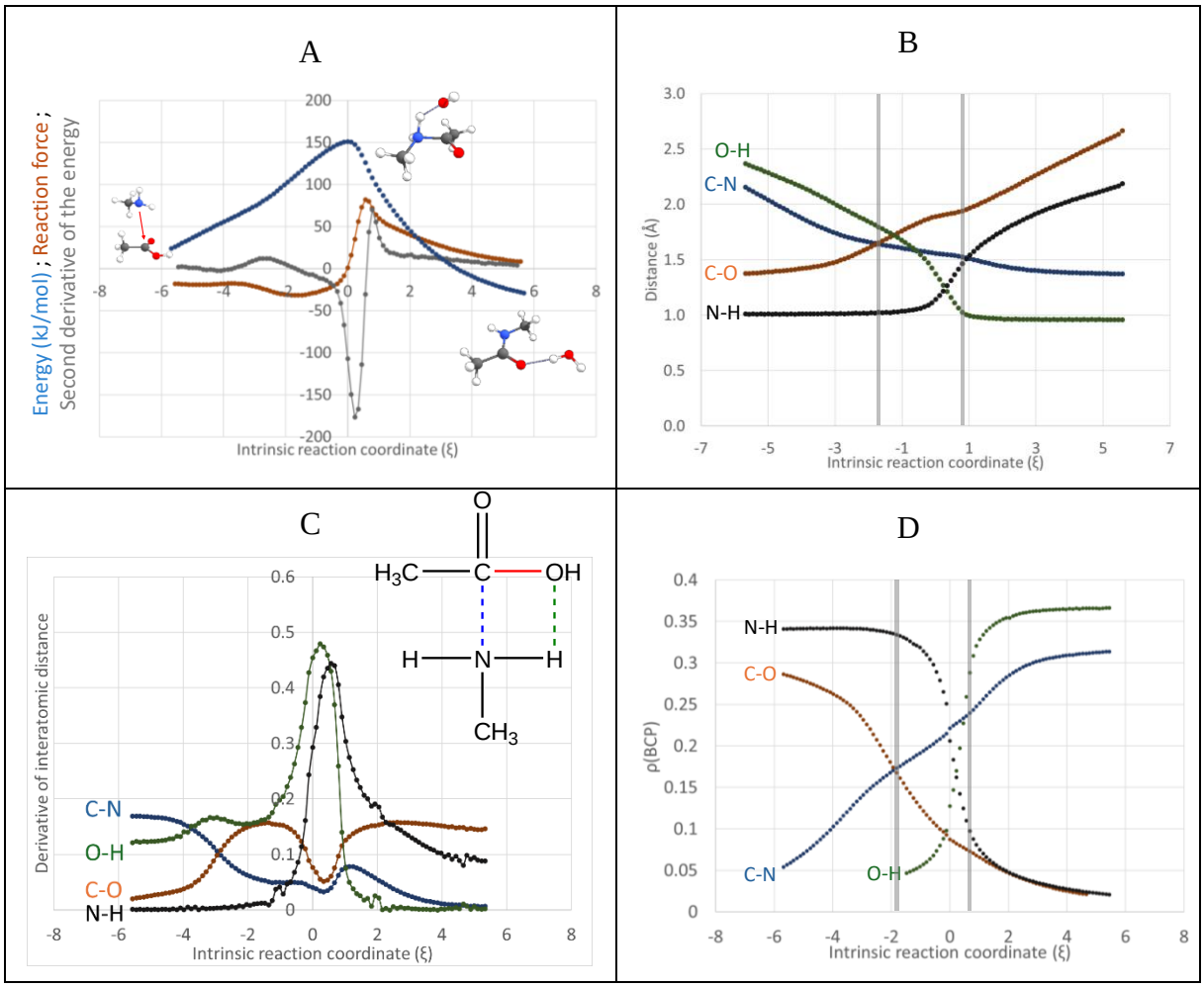

Figure 1: Analysis of the reaction mechanism $CH_3COOH + NH_2CH_3 \rightarrow CH_3CONHCH_3$ in one step without water molecule. Variations, along the intrinsic reaction coordinate, of :A: energy, reaction force and second derivative of energy; B: interatomic distances, C: derivatives of interatomic distances, and D: electron densities at BCP points of bonds. The vertical grey lines divide the reaction path into three regions as defined by the minima and maxima of the reaction force: the regions of the reactants, the transition state and the products, respectively.

The overall evolution of the four interatomic distances of interest (C-O, N-H, C-N, and O-H) is presented in Figure 1B. It is observed that the C-N distance changes significantly in the reactant region. This bond evolves the most in this region, and the C-N distance appears to stabilize in

the transition state region to reach a plateau in the product region. The O-H interatomic distance also begins to decrease in the reactant region. This approach of the O and H atoms intensifies in the transition state region to reach a plateau in the transition state region, corresponding to the formation of the O-H bond. The C-O interatomic distance is initially quite stable in the reactant region and begins to increase towards the end of the reactant region. This increase in the C-O distance, corresponding to the bond breakage, continues in the transition state region and then in the product region. The N-H interatomic distance is very stable in the reactant region. It starts to increase in the transition state region and continues to increase in the product region, corresponding to the rupture of the N-H bond. The study of the derivatives of these interatomic distances along the intrinsic reaction coordinate is quite interesting for highlighting these changes (Figure 1C): $\frac{\partial d_{C-N}}{\partial \zeta}$ evolves significantly in the reactant region. $\frac{\partial d_{C-O}}{\partial \zeta}$ also evolves in this region and continues its evolution in the transition state region. In contrast, the derivatives of the O-H and N-H interatomic distances mainly evolve in the transition state region.

The evolution of the electronic density at the BCPs of these different bonds fully confirms these changes (Fig 1 D), with the formation of the C-N bond characterized by an increase in electronic density at the corresponding BCP. These interactions between the C and N atoms increase significantly in both the reactant and transition state regions, reaching a plateau in the product region. Conversely, the electronic density at the BCP of the C-O bond decreases significantly in the reactant and transition state regions, leading to the rupture of this interaction in the product region. The evolution of the N-H and O-H interactions clearly occurs in the transition state region, with an N-H bond that is stable in the reactant region and breaks in the transition state region, and conversely, an O-H bond that is non-existent in the reactant region, forming in the transition state region and leading to the elimination of the water molecule in the product region.

To complement these analyses, we studied the variations of the Laplacians of the electronic densities at the BCPs of these 4 bonds to identify bond formations and breakages: covalent interactions become non-covalent when the Laplacian of the electronic density changes from negative to positive values, and vice versa. These variations in the Laplacians of the electronic densities are presented in Figure 2, along with the normalized second derivative of the energy $\frac{\partial^2 E}{\partial \zeta^2}$. The superposition of these different curves shows that the formation of the C-N bond is characterized by the transition from a zero to a positive value of $\frac{\partial^2 E}{\partial \zeta^2}$. This formation of the C-N bond clearly occurs in the reactant region. For an intrinsic reaction coordinate value of -1.6, the second derivative $\frac{\partial^2 E}{\partial \zeta^2}$ changes sign and becomes negative, corresponding to the entry into the transition state region. This point also corresponds to the breaking of the C-O bond at the level of acetic acid. Then, the formation of the O-H bond and the breaking of the N-H bond occur in the transition state region. The formation of the C-N bond thus appears to be the starting point of the reaction, occurring even before the transition state region, suggesting that the non-bonding pair on the nitrogen atom attacks the π-hole of the carbonyl group very early in the reaction mechanism.

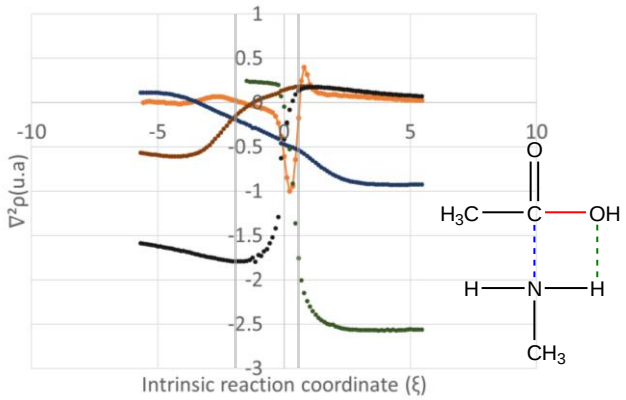

Figure 2: Analysis of the $CH_3COOH + NH_2CH_3 \rightarrow CH_3CONHCH_3$ one-step reaction mechanism without water molecule. Variations, along the intrinsic reaction coordinate, of the Laplacians of the electron density at the BCP points of the two bonds that form (C-N and O-H) and the two bonds that break (C-O and N-H). The second derivative of the normalized energy is also superimposed on this graph in orange. The vertical grey lines divide the reaction path into three regions as defined by the minima and maxima of the reaction force: the regions of the reactants, the transition state and the products, respectively.

The ELF analysis is very useful for confirming this interpretation, as this approach allows for the characterization of electronic pairs, particularly disynaptic valence basins corresponding to covalent bonds, and monosynaptic valence basins corresponding to non-bonding pairs. Figure 3 confirms that the non-bonding pair on the nitrogen atom attacks the π-hole of the carbonyl group to form the C-N bond in the reactant region. The proton transfer from the transient structure to the hydroxyl group occurs in the transition state region.

It is worth underlying that the C=O bond remains virtually unchanged throughout the reaction.

Reagent	Minimium of reaction force	Transition state	Maximum of reaction force	Product
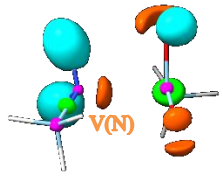	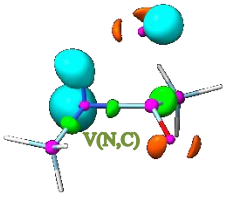	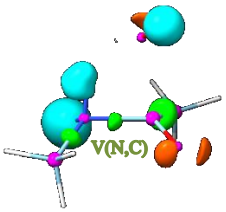	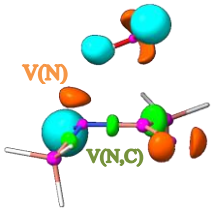	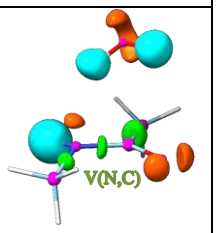
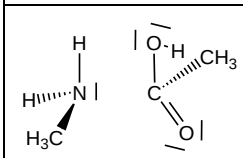	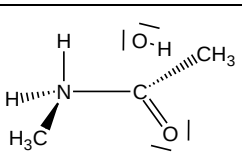	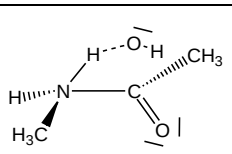	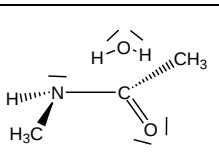	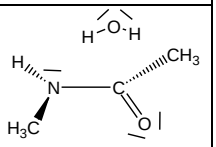

Figure 3: Evolution of the core and valence basins as defined by ELF analysis at the characteristic points of the reaction, for the one-step formation of methylacetamide in the absence of a water molecule, and interpretation in terms of Lewis structures. Basins colored in orange, green and cyan represent monosynaptic V(X) basins, disynaptic V(X,Y) basins, and monosynaptic protonated basins, respectively.

c. Effect of the addition of water molecules

All the reaction paths discussed in the following are shown in Figure 4.

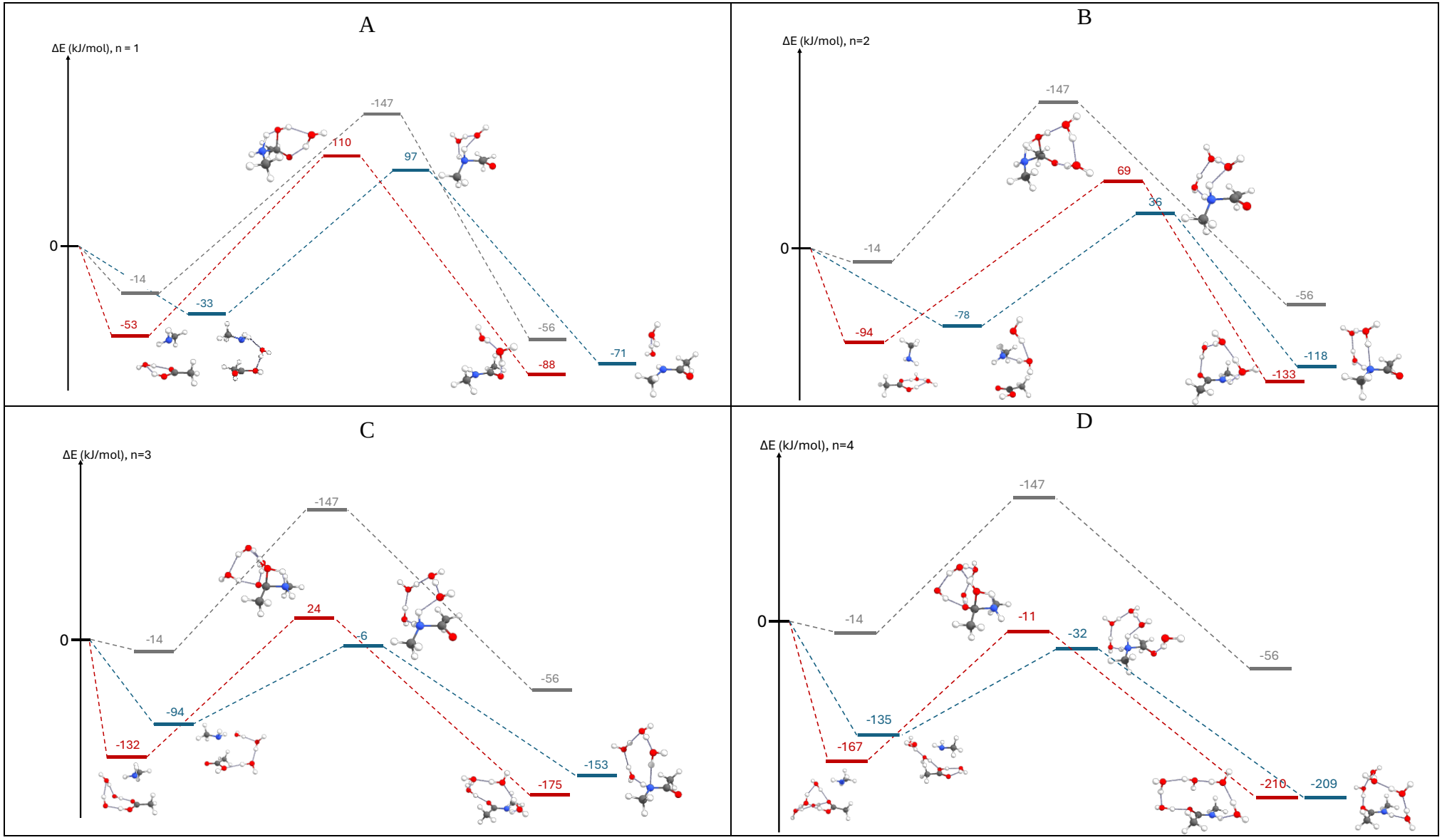

Figure 4: Identification of the different reaction profiles for the one-step formation of methylacetamide from methylamine and acetic acid in the presence of 1, 2, 3 and 4 water molecules (figures A, B, C and D, respectively). The pathways shown in red and blue correspond to the microhydration of acetic acid and the transition state, respectively. The pathway shown in gray corresponds to the pathway without the presence of a water molecule. The energies of the stationary points have been calculated with reference to those of all the reactants taken separately (n(H_2O) + CH_3COOH + NH_2CH_3).

The "net energy barriers" required to reach the transition state from the complex formed from the isolated reactants are given in Table 1, as a function of the number of water molecules of hydration and the type of microhydration (microhydration of reactants versus microhydration of TS). Among others, it is worth mentioning that microhydration of the reactant does not lower the barrier, but it lowers the TS energy by approximately 40 kJ/mol.

Number of water molecules	Micro-hydration of	$E_{complex}$ (kJ/mol)	$E_{transition\_State}$ (kJ/mol)	$E_{products}$ (kJ/mol)	$\Delta E = E_{transition\_State} - E_{complex}$ (kJ/mol)
0		-14	147	-56	161
1	Acetic acid	-53	110	-88	163
	Transition State	-33	97	-71	130
2	Acetic acid	-94	69	-63	163
	Transition State	-78	36	-118	114
3	Acetic acid	-132	24	-175	156
	Transition State	-94	-6	-153	88
4	Acetic acid	-167	-11	-210	156
	Transition State	-135	-32	-209	103

Table 1: "Net energy barriers" required to reach the transition state from the complex formed from the isolated reactants for reaction paths shown in Figure 4.

All the corresponding Cartesian Coordinates of the optimized structures are given in Supplementary Materials.

i. Reaction between micro-hydrated acetic acid and methylamine

The influence of micro-hydration on the reaction force is shown in Figure 5A, corresponding to the reaction mechanisms involving micro-hydrated acetic acid (mechanism shown in red in Figure 4).

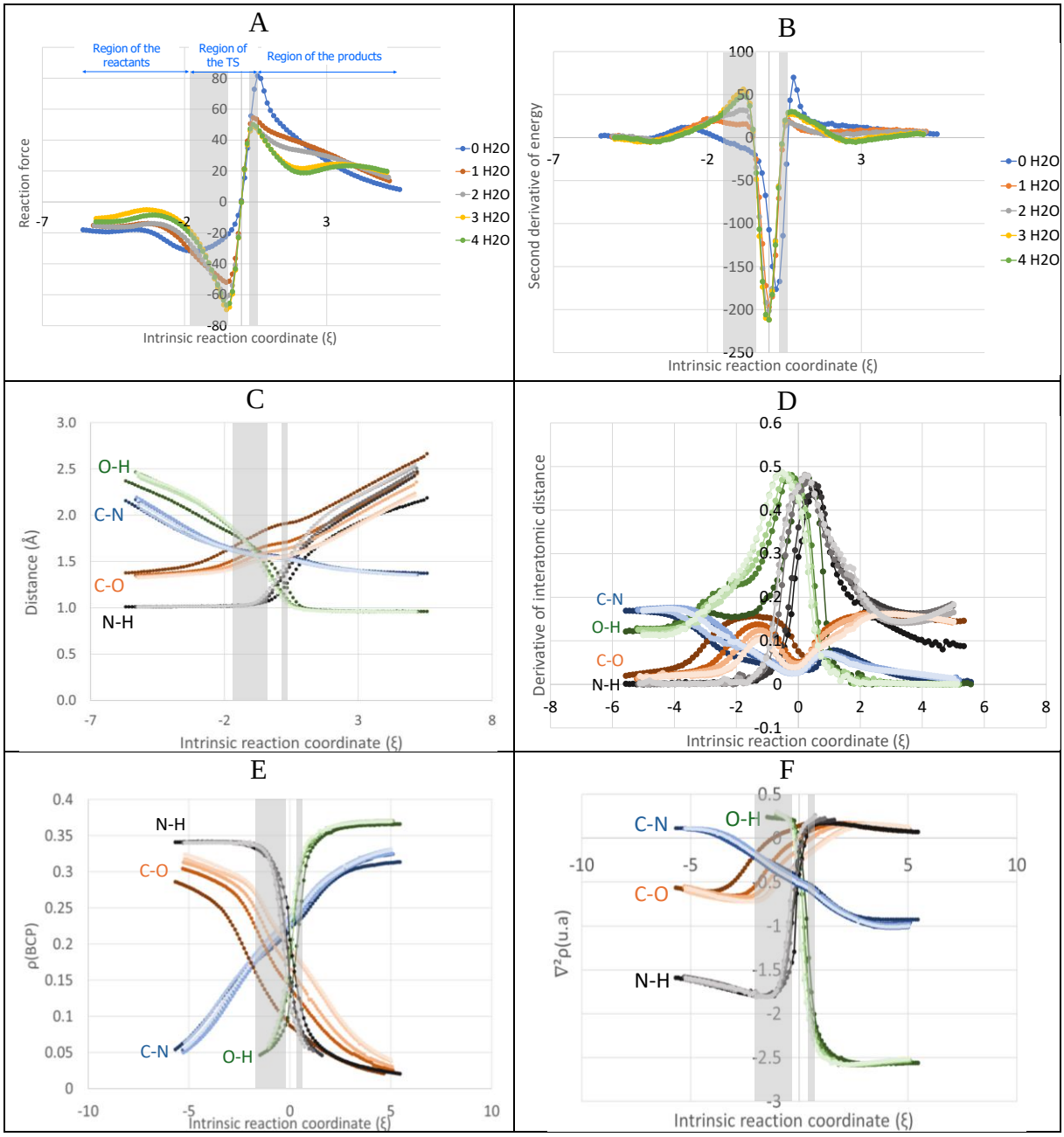

Figure 5: Influence of microhydration of acetic acid prior to its one-step reactif with methylamine. Variations, along the intrinsic reaction coordinate, of: A: reaction force, B: second derivative of energy; C: interatomic distances, D: derivatives of interatomic distances, E: electron densities at the BCP points of the 4 bonds of interest, and F: Laplacian of the electron density at the BCP points of the 4 bonds of interest. The vertical grey marks divide the reaction path into three regions as defined by the minima and maxima of the reaction force: the regions of the reactants, the transition state and the products, respectively. The different regions are shown in the case of the reaction mechanism without water molecules. The exact positions of these limits, depending on the number of water molecules, are given in Table 2.

Overall, the presence of a single water molecule hydrating acetic acid prior to its reaction with methylamine strongly shortens the region of the reactants, and lengthens the region of the transition state. On the other hand, the variation in reaction force along the intrinsic reaction coordinate is little affected when further water molecules are added. (Table 2).

n	Region of the reactants	Region of the transition state	Region of the products
0	$\zeta < -1.82$	$-1.82 < \zeta < 0.68$	$0.68 < \zeta$
1	$\zeta < -0.42$	$-0.42 < \zeta < 0.53$	$0.53 < \zeta$
2	$\zeta < -0.42$	$-0.42 < \zeta < 0.53$	$0.53 < \zeta$
3	$\zeta < -0.52$	$-0.52 < \zeta < 0.42$	$0.42 < \zeta$
4	$\zeta < -0.52$	$-0.52 < \zeta < 0.31$	$0.31 < \zeta$

Table 2: Division of the reaction paths into three regions as defined by the minima and maxima of the reaction force, depending on the number n of water molecules, in the case of the reaction mechanisms shown in red, Figure 4.

As more water molecules are added, the increase in the C-O distance is delayed and occurs primarily in the transition state region rather than in the product region. Other interatomic distances are little affected by the presence of water molecules (Figure 5C). This variation is clearly visible in the curves showing the derivative of the interatomic distance (Figure 5D), with the delay of the C-O breaking bond. The study of the variations in electronic density and its Laplacian at the 4 BCPs of the bonds of interest confirms this (Figure 5E, F):

- the formation of the C-N bond always occurs first, in the reactant region, as observed without water molecules,
- the presence of water molecules delays the breaking of the C-O bond, which no longer occurs in the reactant region but in the transition state region, starting with the presence of just one water molecule,
- the presence of water molecules does not affect the evolution of the N-H and O-H bonds, which are broken and formed, respectively, in the transition state region.

The delay in breaking the C-O bond is also highlighted by ELF analysis (Figure 6):

- without a water molecule, the disynaptic valence pool corresponding to the C-O bond had disappeared at the transition state,
- in the presence of a single water molecule, this pool still exists at maximum reaction force, i.e. right up to the product region.

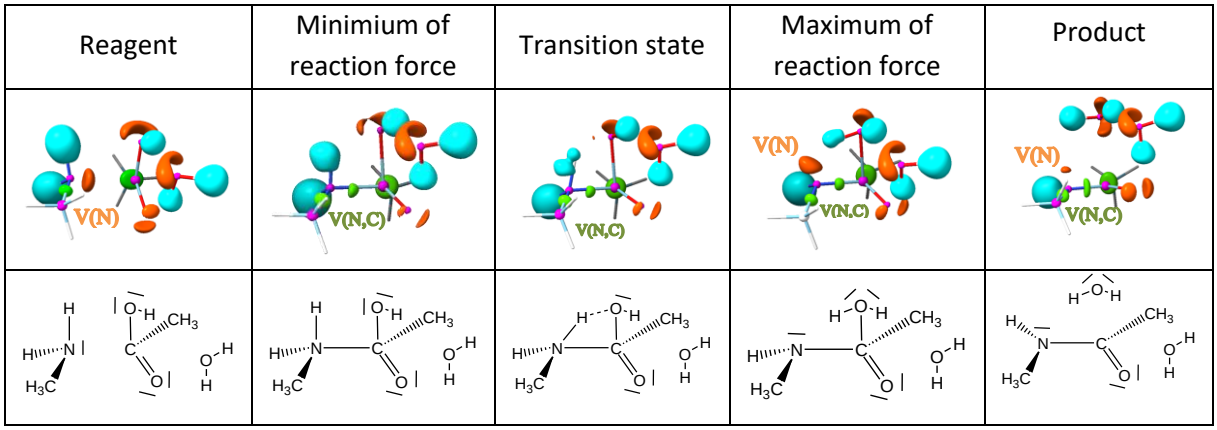

Figure 6: Evolution of the core and valence basins as defined by ELF analysis at the characteristic points of the reaction, for the one-step formation of methylacetamide in the presence of a molecule of water of hydration on acetic acid prior to its reaction, and interpretation in terms of Lewis structures. Basins colored in orange, green and cyan represent monosynaptic V(X) basins, disynaptic V(X,Y) basins, and monosynaptic protonated basins, respectively.

ii. Stabilizing the transition state with water molecules

When water molecules are placed to maximize the stabilization of the transition state, the lowering of the reaction potential energy is more significant, approximately 15, 30, 30, and 20 kJ/mol with the presence of 1, 2, 3, and 4 water molecules, respectively, compared to micro-hydration of acetic acid. This micro-hydration, which maximally stabilizes the transition state and thus further lowers the energy barrier, corresponds to positioning water molecules between the carbonyl group of acetic acid and the amine group of methylamine. Such micro-hydration naturally disrupts the formation and breaking of the 4 bonds of interest since they involve atoms from the carbonyl group of acetic acid and/or atoms from the amine group of methylamine. This is evident in Figure 7 :

- the C-N bond forms even earlier in the reactant region,
- the C-O bond is broken earlier, in the reactant region, but still after the formation of the C-N bond,
- the proton transfer from the amine to the hydroxyl group still occurs in the transition state region.

The presence of just one water molecule is sufficient for these modifications, and adding additional water molecules has a lesser effect on the reaction mechanism. In terms of force and second derivative of the energy, the presence of one water molecule results in the following position of the region of the reactants, transition state and products: $-8.8 < \zeta < -3.5$ for the reagents, $-3.5 < \zeta < 1.9$ for the transition state and $1.9 < \zeta < 8.6$ for the products, respectively (Table 3). On the other hand, the presence of 2 to 4 water molecules will slightly displace these regions and looks similar (reactant region for $-9.5 < \zeta < -2.6$, transition state region for $-2.6 < \zeta < 1.4$, and product region $1.4 < \zeta < 9.2$).

n	Region of the reactants	Region of the transition state	Region of the products
0	$\zeta < -1.82$	$-1.82 < \zeta < 0.68$	$0.68 < \zeta$
1	$\zeta < -3.51$	$-3.51 < \zeta < 1.94$	$1.94 < \zeta$
2	$\zeta < -2.92$	$-2.92 < \zeta < 2.33$	$2.33 < \zeta$
3	$\zeta < -2.36$	$-2.36 < \zeta < 2.16$	$2.16 < \zeta$
4	$\zeta < -2.65$	$-2.65 < \zeta < 1.23$	$1.23 < \zeta$

Table 3: Division of the reaction paths into three regions as defined by the minima and maxima of the reaction force, depending on the number n of water molecules, in the case of the reaction mechanisms shown in blue, Figure 4.

ELF analysis at the relevant points along the reaction pathway in the presence of a water molecule of hydration of the transition state is presented in Supplementary Material. In terms of ELF basins, this analysis is not very different from that obtained without water molecules, with the C-N bond formed at the minimum of the reaction force, the C-O bond broken for the transition state, and the proton transfer observed at the maximum of the reaction force.

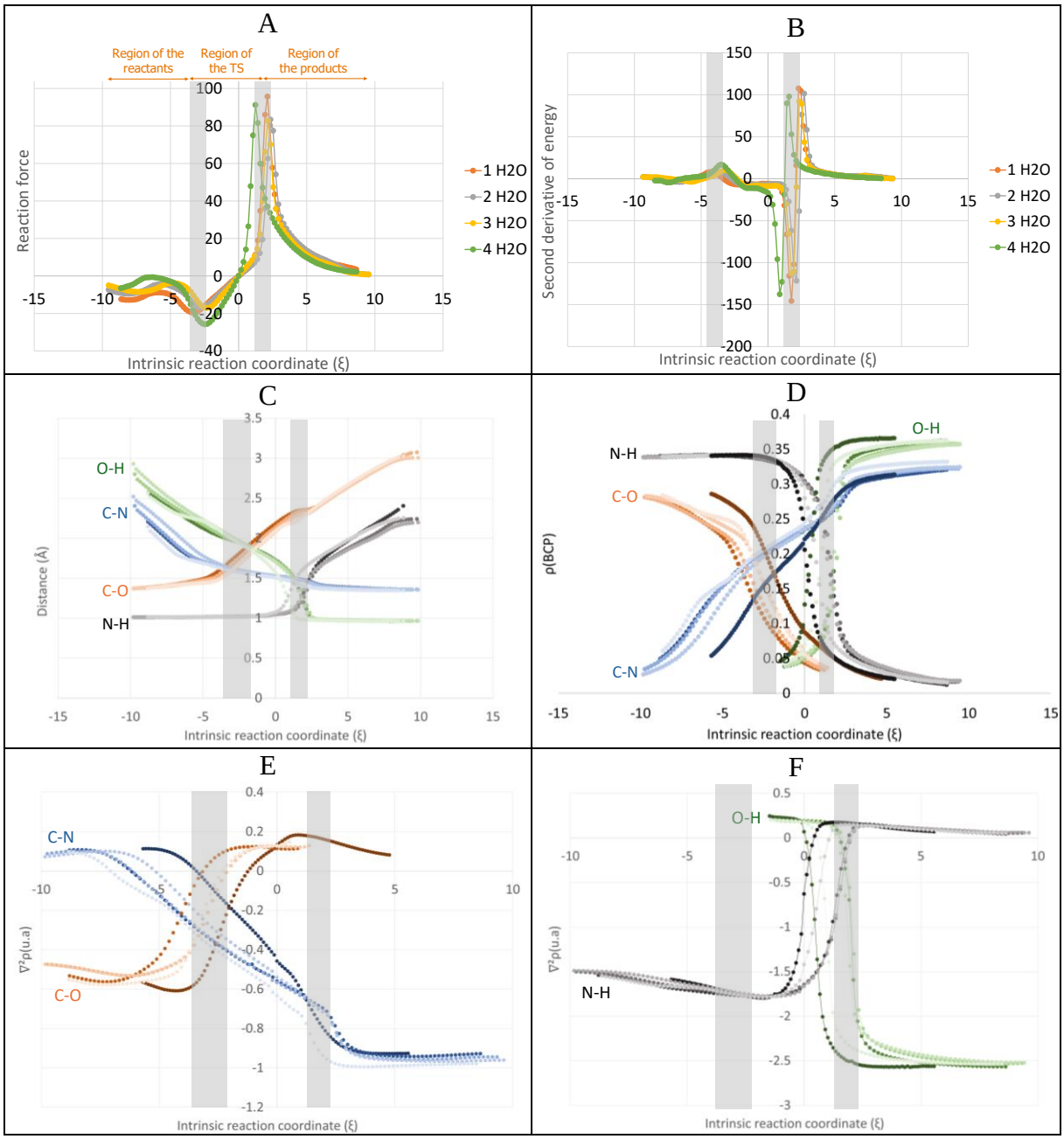

Figure 7: Influence of micro-hydration on the transition state for the $CH_3COOH + NH_2CH_3 \rightarrow CH_3CONHCH_3$ one-step reaction mechanism. Variations, along the intrinsic reaction coordinate, of : A: reaction force, B : second derivative of energy; C: interatomic distances; D: electron densities at BCP points of the 4 bonds of interest, and E and F: Laplacian of electron density at BCP points of the 4 bonds of interest. . The vertical grey marks divide the reaction path into three regions as defined by the minima and maxima of the reaction force: the regions of the reactants, the transition state and the products, respectively. The different regions are shown in the case of the reaction mechanism with one water molecules. The exact positions of these limits, depending on the number of water molecules, are given in Table 3.

V. Conclusion and perspectives

The evolution of the system's energy, interatomic distances, as well as electronic densities and their derivatives throughout the reaction, are key quantities for studying reaction mechanisms. Their joint study allows for describing bond formations and breakages in terms of electronic redistributions within the system.

In this work, we compared the effects of two micro-hydration patterns on a single-step reaction involving the formation of two bonds and the breaking of two bonds: the formation of methylacetamide from methylamine and acetic acid, considering either the micro-hydration of acetic acid prior to its reaction or the micro-hydration at the transition state.

Without water molecules, the C-N bond forms very early in the reaction process, in the transition state region. Then, the C-O bond is broken. Finally, the proton migration from the amine group to the hydroxyl group occurs in the transition state region.

Micro-hydration of acetic acid prior to its reactivity lowers the overall reaction potential energy. It appears to have little effect on the formation of the C-N bond. However, it delays the breaking of the C-O bond, which occurs in the transition state region, similar to the proton migration from the amine group to the hydroxyl group.

Micro-hydration of the transition state allows for a further decrease in the overall reaction potential energy. Electronic redistribution is also more significantly affected by this micro-hydration, leading to earlier formation of the C-N bond and earlier breaking of the C-O bond, in the reactant region.

This approach, based on the joint study of different energetic, geometric, and topological quantities, as well as their derivatives, seems highly relevant for describing the influence of non-covalent interactions on the reactivity of chemical species. Furthermore, introducing new derivatives by analogy with classical physics approaches, such as the reaction force introduced by A. Torro Labbé et al. in the 2000s, or the derivative of interatomic distances, appears quite pertinent for describing the influence of non-covalent interactions on reactivity. The methodology implemented here could certainly be applied to other reaction processes, such as in interstellar media or atmospheric chemistry. Notably, it will be very interesting to determine whether non-covalent interactions leading to shifted electronic redistributions in the reactant region are systematically associated with a greater lowering of reaction enthalpies or not.

Funding

We would like to thank the ED388 doctoral school (chimie-physique et chimie analytique de Paris Centre) for its funding of Olivier Aroule's thesis.

References

[1] Herbst, E., & Garrod, R. T. (2022). Synthetic approaches to complex organic molecules in the cold interstellar medium. *Frontiers in Astronomy and Space Sciences*, *8*, 789428.

[2] Tinacci, L., Ferrada-Chamorro, S., Ceccarelli, C., Pantaleone, S., Ascenzi, D., Maranzana, A., Balucani, N. & Ugliengo, P. (2023). The GRETOBAPE gas-phase reaction network: the importance of being exothermic. *The Astrophysical Journal Supplement Series*, *266*(2), 38.

[3] Tonolo, F., Lupi, J., Puzzarini, C., & Barone, V. (2020). The quest for a plausible formation route of formyl cyanide in the interstellar medium: A state-of-the-art quantum-chemical and kinetic approach. *The Astrophysical Journal*, *900*(1), 85.

[4] Puzzarini, C. (2022). Gas-phase chemistry in the interstellar medium: The role of laboratory astrochemistry. *Frontiers in Astronomy and Space Sciences*, *8*, 811342.

[5] Strecker, A. (1850). Ueber die künstliche Bildung der Milchsäure und einen neuen, dem Glycocoll homologen Körper. *Justus Liebigs Annalen der Chemie*, 75(1), 27-45.

[6]Riffet, V., Frison, G., & Bouchoux, G. (2018). Quantum-chemical modeling of the first steps of the Strecker synthesis: from the gas-phase to water solvation. The Journal of Physical Chemistry A, 122(6), 1643-1657..

[7] Neelamraju, V. S. K., & Jaganade, T. (2019). A reaction force perspective of a model amide bond formation reaction. *Computational and Theoretical Chemistry*, *1151*, 91-98.

[8] Gale, A. G., Odbadrakh, T. T., Ball, B. T., & Shields, G. C. (2020). Water-mediated peptide bond formation in the gas phase: A model prebiotic reaction. *The Journal of Physical Chemistry A*, *124*(20), 4150-4159.

[9] Kerkeni, B., & Simmie, J. M. (2023). Peptide bonds in the interstellar medium: facile catalytic formation from nitriles on water–ice grains. *The Journal of Physical Chemistry A*, *127*(25), 5382-5389.

[10] Boland, M., Chaquin, P., Volatron, F., & Markovits, A. (2024). Formamide synthesis in the interstellar medium catalyzed by damaged water ice. *Astronomy & Astrophysics*, *682*, A13.

[11] Rimola, A., Sodupe, M., & Ugliengo, P. (2010). Deep-space glycine formation via Strecker-type reactions activated by ice water dust mantles. A computational approach. *Physical Chemistry Chemical Physics*, *12*(20), 5285-5294.

[12] Koch, D. M., Toubin, C., Peslherbe, G. H., & Hynes, J. T. (2008). A theoretical study of the formation of the aminoacetonitrile precursor of glycine on icy grain mantles in the interstellar medium. *The Journal of Physical Chemistry C*, *112*(8), 2972-2980.

[13] Bovolenta, G. M., Silva-Vera, G., Bovino, S., Molpeceres, G., Kästner, J., & Vogt-Geisse, S. (2024). In-depth exploration of catalytic sites on amorphous solid water: I. The astrosynthesis of aminomethanol. *Physical Chemistry Chemical Physics*, *26*(27), 18692-18706.

[14] Rimola, A., Skouteris, D., Balucani, N., Ceccarelli, C., Enrique-Romero, J., Taquet, V., & Ugliengo, P. (2018). Can formamide be formed on interstellar ice? An atomistic perspective. *ACS Earth and Space Chemistry*, *2*(7), 720-734.

[15] Silva-Vera, G., Bovolenta, G. M., Rani, N., Vera, S., & Vogt-Geisse, S. (2024). Pathways to Interstellar Amides via Carbamoyl (NH2CO) Isomers by Radical-Neutral Reactions on Ice Grain Mantles. *ACS Earth and Space Chemistry*, *8*(7), 1480-1494.

[16] Toro-Labbé, A., Gutiérrez-Oliva, S., Murray, J. S., & Politzer, P. (2007). A new perspective on chemical and physical processes: the reaction force. *Molecular Physics*, *105*(19-22), 2619-2625.

[17] Toro-Labbé, A., Gutiérrez-Oliva, S., Murray, J. S., & Politzer, P. (2009). The reaction force and the transition region of a reaction. *Journal of molecular modeling*, *15*, 707-710.

[18] Politzer, P., Toro-Labbé, A., Gutiérrez-Oliva, S., Herrera, B., Jaque, P., Concha, M. C., & Murray, J. S. (2005). The reaction force: Three key points along an intrinsic reaction coordinate. *Journal of Chemical Sciences*, *117*, 467-472.

[19] Bader, R. F. (1985). Atoms in molecules. *Accounts of chemical research*, *18*(1), 9-15.

[20] Popelier, P. L. A. (2014). The QTAIM perspective of chemical bonding. *The chemical bond: fundamental aspects of chemical bonding*, 271-308.

[21] Kutzelnigg, W. (1992). Atoms in Molecules. A Quantum Theory.(Reihe: International Series of Monographs on Chemistry, Vol. 22.) Von RFW Bader. Clarendon Press, Oxford, 1990. XVIII, 438 S., geb.£ 50.00.–ISBN 0-19-855168-1. *Angewandte Chemie*, *104*(10), 1423-1423.

[22] Becke, A. D., & Edgecombe, K. E. (1990). A simple measure of electron localization in atomic and molecular systems. *The Journal of chemical physics*, *92*(9), 5397-5403.

[23] Silvi, B., & Savin, A. (1994). Classification of chemical bonds based on topological analysis of electron localization functions. *Nature*, *371*(6499), 683-686.

[24] Grin, Y., Savin, A., & Silvi, B. (2014). The ELF perspective of chemical bonding. *The Chemical Bond: Fundamental Aspects of Chemical Bonding*, 345-382.

[25] Mehringer, D. M., Snyder, L. E., Miao, Y., & Lovas, F. J. (1997). Detection and confirmation of interstellar acetic acid. *The Astrophysical Journal*, *480*(1), L71.

[26] Kaifu, N., Morimoto, M., Nagane, K., Akabane, K., Iguchi, T., & Takagi, K. (1974). Detection of interstellar methylamine. *Astrophysical Journal, vol. 191, p. L135-L137*, *191*, L135-L137.

[27] Cheung, A. C., Rank, D. M., Townes, C. H., Thornton, D. D., & Welch, W. (1969). Detection of water in interstellar regions by its microwave radiation. *Nature*, *221*(5181), 626-628.

[28] Gaussian 16, Revision C.01, M. J. Frisch, G. W. Trucks, H. B. Schlegel, G. E. Scuseria, M. A. Robb, J. R. Cheeseman, G. Scalmani, V. Barone, G. A. Petersson, H. Nakatsuji, X. Li, M. Caricato, A. V. Marenich, J. Bloino, B. G. Janesko, R. Gomperts, B. Mennucci, H. P. Hratchian, J. V. Ortiz, A. F. Izmaylov, J. L. Sonnenberg, D. Williams-Young, F. Ding, F. Lipparini, F. Egidi, J. Goings, B. Peng, A. Petrone, T. Henderson, D. Ranasinghe, V. G. Zakrzewski, J. Gao, N. Rega, G. Zheng, W. Liang, M. Hada, M. Ehara, K. Toyota, R. Fukuda, J. Hasegawa, M. Ishida, T. Nakajima, Y. Honda, O. Kitao, H. Nakai, T. Vreven, K. Throssell, J. A. Montgomery, Jr., J. E. Peralta, F. Ogliaro, M. J. Bearpark, J. J. Heyd, E. N. Brothers, K. N. Kudin, V. N. Staroverov, T. A. Keith, R. Kobayashi, J. Normand, K. Raghavachari, A. P. Rendell, J. C. Burant, S. S. Iyengar, J. Tomasi, M. Cossi, J. M. Millam, M. Klene, C. Adamo, R. Cammi, J. W. Ochterski, R. L. Martin, K. Morokuma, O. Farkas, J. B. Foresman, and D. J. Fox, Gaussian, Inc., Wallingford CT, 2016.

[29] Derbali, I., Aroule, O., Hoffmann, G., Thissen, R., Alcaraz, C., Romanzin, C., & Zins, E. L. (2022). On the relevance of the electron density analysis for the study of micro-hydration and its impact on the formation of a peptide-like bond. *Theoretical Chemistry Accounts*, *141*(7), 34.

[30] Vydrov, O. A., & Scuseria, G. E. (2006). Assessment of a long-range corrected hybrid functional. *The Journal of chemical physics*, *125*(23).

[31] Vydrov, O. A., Heyd, J., Krukau, A. V., & Scuseria, G. E. (2006). Importance of short-range versus long-range Hartree-Fock exchange for the performance of hybrid density functionals. *The Journal of chemical physics*, *125*(7).

[32] Vydrov, O. A., Scuseria, G. E., & Perdew, J. P. (2007). Tests of functionals for systems with fractional electron number. *The Journal of chemical physics*, *126*(15).

[33]Grimme, S., Ehrlich, S., & Goerigk, L. (2011). Effect of the damping function in dispersion corrected density functional theory. *Journal of computational chemistry*, *32*(7), 1456-1465.

[34] Goerigk, L., Kruse, H., & Grimme, S. (2011). Benchmarking density functional methods against the S66 and S66x8 datasets for non-covalent interactions. *ChemPhysChem*, 12(17), 3421-3433.

[35] Hratchian, H. P., & Schlegel, H. B. (2004). Accurate reaction paths using a Hessian based predictor–corrector integrator. *The Journal of chemical physics*, *120*(21), 9918-9924.

[36] Hratchian, H. P., Schlegel, H. B., Dykstra, C. E., Frenking, G., Kim, K. S., & Scuseria, G. (2005). Theory and applications of computational chemistry: the first 40 years. *Dykstra, CE, 195*.

[37] Hratchian, H. P., & Schlegel, H. B. (2005). Using Hessian updating to increase the efficiency of a Hessian based predictor-corrector reaction path following method. *Journal of chemical theory and computation*, *1*(1), 61-69.

[38] Hernández Mancera, J. P., Núñez-Zarur, F., Gutiérrez-Oliva, S., Toro-Labbé, A., & Vivas-Reyes, R. (2020). Diels-Alder reaction mechanisms of substituted chiral anthracene: A theoretical study based on the reaction force and reaction electronic flux. *Journal of computational chemistry*, *41*(23), 2022-2032.

[39] Díaz, S., Brela, M. Z., Gutiérrez-Oliva, S., Toro-Labbé, A., & Michalak, A. (2017). ETS-NOCV Decomposition of the Reaction Force: The HCN/CNH Isomerization Reaction Assisted by Water. *Journal of Computational Chemistry*, *38*(24), 2076-2087.

[40] Jaque, P., Toro-Labbé, A., Politzer, P., & Geerlings, P. (2008). Reaction force constant and projected force constants of vibrational modes along the path of an intramolecular proton transfer reaction. *Chemical Physics Letters*, *456*(4-6), 135-140.

[41] AIMAll (Version 19.10.12), Todd A. Keith, TK Gristmill Software, Overland Park KS, USA, 2019 (aim.tkgristmill.com)

[42] Silvi, B. (2002). The synaptic order: a key concept to understand multicenter bonding. *Journal of molecular structure*, *614*(1-3), 3-10.

[43] Fuster, F., Sevin, A., & Silvi, B. (2000). Determination of substitutional sites in heterocycles from the topological analysis of the electron localization function (ELF). *Journal of Computational Chemistry*, *21*(7), 509-514.

[44] Kozlowski, D., & Pilme, J. (2011). New insights in quantum chemical topology studies using numerical grid-based analyses. *Journal of computational chemistry*, *32*(15), 3207-3217.

[45] Chevreau, H., & Pilmé, J. (2023). Promising insights in parallel grid-based algorithms for quantum chemical topology. *Journal of Computational Chemistry*, *44*(16), 1505-1516.

[46] Derbali, I., Aroule, O., Hoffmann, G., Thissen, R., Alcaraz, C., Romanzin, C., & Zins, E. L. (2022). On the relevance of the electron density analysis for the study of micro-hydration and its impact on the formation of a peptide-like bond. *Theoretical Chemistry Accounts*, *141*(7), 34.

[47] Murray, J. S., Lane, P., Clark, T., Riley, K. E., & Politzer, P. (2012). σ-Holes, π-holes and electrostatically-driven interactions. *Journal of molecular modeling*, *18*, 541-548.

[48] Murray, J. S., & Politzer, P. (2017). Molecular electrostatic potentials and noncovalent interactions. *Wiley Interdisciplinary Reviews: Computational Molecular Science*, *7*(6), e1326.

[49] Politzer, P., Murray, J. S., & Clark, T. (2010). Halogen bonding: an electrostatically-driven highly directional noncovalent interaction. *Physical Chemistry Chemical Physics*, *12*(28), 7748-7757.